Mitigating the Urban Heat Island Phenomenon Using a Water-Retentive Artificial Turf System

Tebakari, Taichi
Associate Prof., Dept. of Environmental Engineering, Toyama Prefectural University, Japan

Maruyama, Tatsuya
Ito Land Readjustment Office, Housing & Urban Planning Bureau of Fukuoka City

Inui, Masahiro
Prof., Faculty of Sports and Health Science, Fukuoka University

ABSTRACT: To investigate the thermal properties of a water-retentive artificial turf system (W-ATS), we estimated hydrologic parameters including thermal conductivity, heat capacity, and surface albedo for both the W-ATS and natural grass. We used a model experiment to measure surface temperature and evaporation for both the W-ATS and natural grass. We found that the W-ATS had lower thermal conductivity than natural grass did, and it was difficult for the W-ATS to convey radiant heat to the ground. Compared to natural grass, the W-ATS also had lower heat capacity, which contributed to its larger variation in surface temperature: the W-ATS had higher surface temperatures during daytime and lower surface temperatures during nighttime. The albedo of the W-ATS was one-quarter that of natural grass, and reflected shortwave radiation from the W-ATS surface was lower than that from the surface of natural grass. These results indicate that the W-ATS caused the soil temperature to increase. Furthermore, evaporation from the W-ATS was one-quarter the value of evapotranspiration from natural grass.

1 INTRODUCTION

Recently, the urban heat island (UHI) phenomenon, in which air temperatures are higher in urban areas than in rural areas, has become a serious problem in Japanese mega-cities. Air temperatures differ most between urban and rural areas during nighttime. Over the last 100 years, daily minimum temperatures have increased by about 3.8°C in Japanese mega-cities (Sapporo, Sendai, Tokyo, Nagoya, Kyoto, and Fukuoka) and by about 1.5°C in medium and small cities (JMA 2005).

Increasingly hot, humid nights have resulted in socioeconomic problems, increased incidence of heat disorder, and increased energy consumption (Ministry of Environment 2005). In addition, the UHI phenomenon may trigger concentrated heavy rains and possibly urban flooding (Mikami 2005). Dixon and Mote (2003) explained the relationship between the atmospheric environment and the UHI phenomenon, and suggested that the UHI phenomenon could be the cause of 'air bump' and urban heavy rainfall.

Many researchers have studied ways to mitigate UHIs, including rooftop gardening and application of permeable pavement and high-reflectance coatings (Kinouchi et al. 1999; Hirano et al. 2004; Murakami et al. 2007). Ichinose et al. (2006) estimated the efficiency of rooftop gardening using experimental measurements, and found that gardens could decrease sensible heat flux by half. Kato et al. (2007) investigated atmospheric cooling through the use of river water, in which every citizen participated in 'uchimizu' (a custom of sprinkling water on the streets) as a communal activity. Kano et al. (2004) conducted numerical simulations and a social experiment

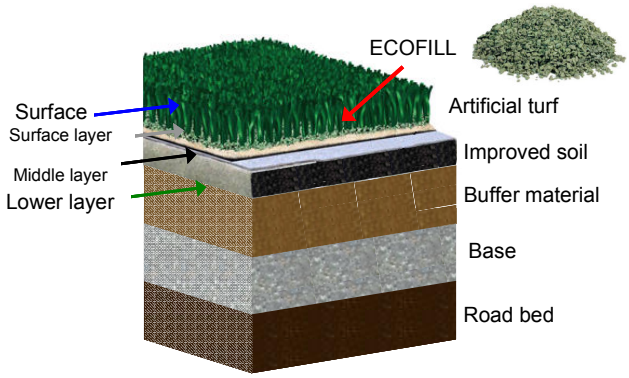

Fig. 1. Schematic of the artificial turf setup.

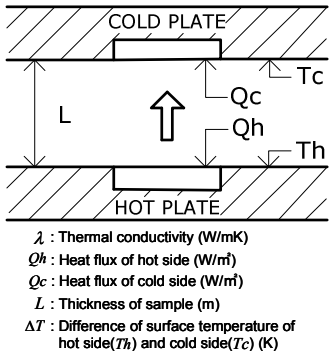

Fig. 2. Schematic of measurement principles of thermal conductivity.

called "uchimizu operation," and estimated that uchimizu could decrease air temperature by 2–2.5°C.

Fukuoka University installed a soccer field of water-retentive artificial turf with the goal of controlling urban flooding and mitigating the thermal environment in an urban area. Immediately after installation, hydrological observations were conducted; measurements revealed that air temperatures and specific humidity above the artificial turf system were equal to those above natural grass (Tebakari et al. 2008).

In this study, coefficients of thermal conductivity, heat capacity, and albedo of artificial turf and natural grass were estimated to clarify the thermal environmental properties of artificial turf. In addition, temperature profiles and evapotranspiration were measured and compared for artificial turf and natural grass using a model experiment.

2 ARTIFICIAL TURF SYSTEM AND NATURAL GRASS

2.1 Soccer field using an artificial turf system

Fig. 1 shows a schematic of a soccer field using our proposed artificial turf system, which is composed of four layers. The upper layer is a water-retentive artificial turf (Mondo Turf Fine Tuned System, Mondo S.P.A., Italy; hereafter 'artificial turf'). The artificial turf consists of two prominent layers. The lower layer of the artificial turf is a buffer material ('Fine Tuned'), made from recycled scrap tires. 'Fine Tuned' provides shock absorption and water retention, enabling constant moistness. The upper layer of the artificial turf is constructed of polyethylene resin grass. The surface layer was processed with an ultraviolet (UV) demulcent to protect it from UV light. River sand (10 kg/m^2) and Ecofill (8 kg/m^2), a patented polyolefin-based granule, were also used as fill for the artificial turf.

Highly permeable and retention-improved soil was installed in the lower layer of our artificial turf system using a construction method that improves permeability and retention by combining soil with a chemical admixture that changes the aggregate structure.

2.2 Natural grass in this study

The grasses in this study included 'Victor' (Japanese grass, natural grass A, February–June 2008), an admixture of tall fescue, Kentucky bluegrass, and perennial ryegrass (Western grass, natural grass B, June–August 2008), and an admixture of Tifton and perennial ryegrass (Western grass,

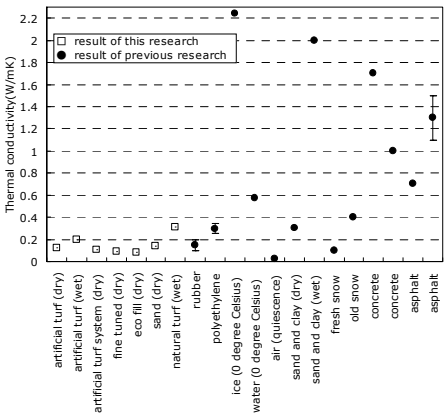

Fig. 3. Comparison of measurement results for thermal conductivity: artificial turf material, natural grass, and results of previous research (Kondo, 1994; Chronological scientific table, 2008).

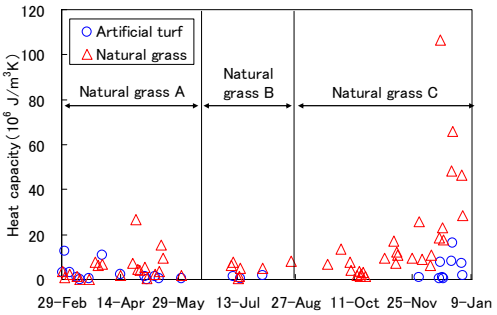

Fig. 4. Time series of heat capacity for artificial turf and natural grass from February 29–November 14, 2008.

natural grass C, August–November 2008). Each experimental plot was 1 m^2 in size. All samples were installed on the roof of a two-story laboratory. A carpeted heat-insulating agent was installed between the roof surface and experimental samples, and water was sprinkled on both natural grass and artificial turf every morning at 9:00 a.m.

3 OBSERVATIONAL AND EXPERIMENTAL METHODS

3.1 Coefficient of thermal conductivity

Fig. 2 presents a schematic diagram of measurement principles for thermal conductivity. Coefficients of thermal conductivity for artificial turf and natural grass were measured using a thermal conductivity measuring device (HC-074, produced by Eko Instruments Co., Ltd.). This device employs a heat flow meter method (steady state method), according to the standards guidelines set out by ASTM-518, ISO-8301, and JIS-1412-Part 2. Standard calibration values were determined using standard reference material (SRM)-1450B from the National Institute of Standards and Technology (NIST).

Fine-grained and moisture materials (artificial turf, natural grass, Ecofill, and sand) were wrapped in transparent polyethylene. In this paper, 'artificial turf' means artificial turf with fill of sand and Ecofill. The transparent polyethylene did not affect the measuring results of thermal conductivity.

The coefficient of thermal conductivity for the artificial turf system (artificial turf combined with Fine Tuned) was calculated based on thermal resistance. Thermal resistance (R m^{2}K/W) describes heat transference and can be expressed as L/λ using the coefficient of thermal conductivity λ and thickness L. The following equations were used to determine the coefficient of thermal conductivity for the artificial turf system:

$$R_t = R_a + R_f = \frac{L_a}{\lambda_a} + \frac{L_f}{\lambda_f} \quad (1)$$

$$\lambda_t = \frac{L_t}{R_t} \tag{2}$$

where suffix t is the artificial turf system, a is the artificial turf, and f is Fine Tuned.

3.2 Heat capacity

As one of the physical properties that affects surface temperature, heat capacity was calculated using the following equations (Kondo 1994):

$$Rn_0 = \sigma T_0^4 - L_0^{\downarrow} \tag{3}$$

$$L^{\downarrow} = (0.74 + 0.19\alpha + 0.07\alpha^2)\sigma T^4 \tag{4}$$

$$\alpha = \log_{10} \omega_{TOP}* = 0.0315 T_{DEW} - 0.1836 \tag{5}$$

$$DT_{MAX} = T_0 - T_{RAD} \tag{6}$$

$$T_0 - T_S = DT_{MAX} \times P(x) \tag{7}$$

$$P(x) \fallingdotseq 2\pi^{-\frac{1}{2}} x^{\frac{1}{2}} - x + (4/3)\pi^{-\frac{1}{2}} x^{\frac{3}{2}} - (1/2)x^2 + (1/3)\pi^{-\frac{1}{2}} x^{\frac{5}{2}} \quad (x \leqq 0.2) \tag{8}$$

$$P(x) \fallingdotseq \frac{0.001 + 1.168x^{1/2} + x}{1.062 + 1.725x^{1/2} + x} \quad (0 < x \leqq 64) \tag{9}$$

$$P(x) \fallingdotseq \frac{x^{1/2} - 0.498}{x^{1/2} + 0.067} \quad (64 \leqq x \leqq 10^4) \tag{10}$$

$$x = \frac{(4\sigma T_0^{\,3})^2 t}{c_G \rho_G \lambda_G} \tag{11}$$

where Rn_0 is net radiation in early evening (W/m^2), σ is the Stefan-Boltzmann constant (5.67×10^{-8} W/m^{2}K^4), T_0 is the surface temperature in the early evening (K), $L_0^{\downarrow}$ is the downward longwave radiation in the early evening, T is the air temperature (K), $\omega_{TOP}*$ is the available water vapor content (mm), T_{DEW} is the dew-point temperature (deg), T_{RAD} is the limit value of minimum temperature (K), $c_G\rho_G$ is the heat capacity (J/m^{3}K), λ is the coefficient of thermal conductivity (W/mK), T_S is the surface temperature at sunrise (K), x is dimensionless time, and t is nighttime (s).

3.3 Albedo

Albedo is an important parameter affecting land surface behavior. An albedo meter was installed at a height of 5 cm above the artificial turf (1 x 1 m) for two days and at a height of 10 cm for three days in August 2008. The albedo meter was an illuminometer (ML-020S-O, produced by Eko Instruments Co., Ltd.) that recorded measurements at 1-min intervals.

3.4 Surface layer temperature

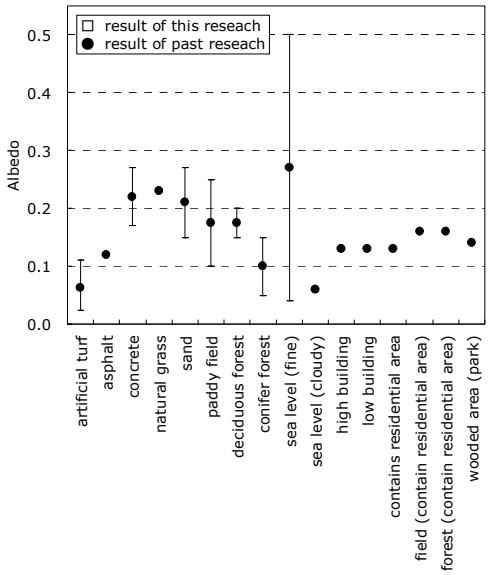

Fig. 5. Comparison of measurement results for the albedo between the artificial turf and past research (Kondo, 1994; Sugawara, 2001).

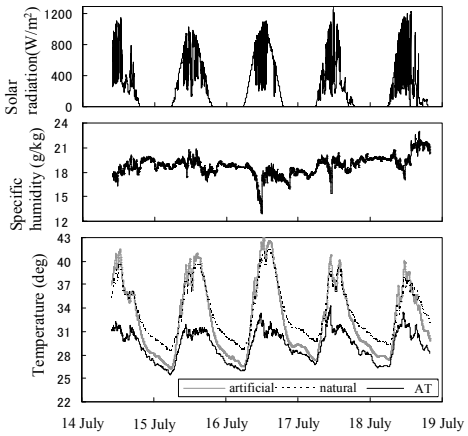

Fig. 6. Time series of solar radiation, specific humidity, and surface temperature for the artificial turf and natural grass, and air temperature from July 14–19, 2008.

Surface layer temperatures of the artificial turf and natural grass were measured using a platinum resistance thermometer (R&D Corporation). 'Surface layer' refers to the level at the roots of grasses, due to protection from direct radiation. The thermometer was installed at a 5-cm depth from the surface of the artificial turf and at a 1-cm height above the soil of natural grass. Observations were conducted from February 29–November 14, 2008. Global solar radiation was measured using a MS-601 pyranometer (Eko Instruments Co., Ltd.), and air temperature and humidity were measured using a HOBO H8 Pro data logger (Onset Computer Corporation).

3.5 Evaporation

3.5.1 Evaporation from artificial turf and natural grass

In this study, it was too difficult to separate the evapotranspiration from natural grass into evaporation and transpiration. Therefore, we compared evaporation from artificial turf with evapotranspiration from natural grass. We constructed an experimental model (20 x 20 cm) that could discharge water from an acrylic undersurface. In the initial condition, both natural grass and artificial turf were sprinkled with water until they were wet. Then, we measured the model's weight every 30 minutes; the difference in weight was used as an indicator of the evaporation rate. A 'wet' condition indicated that water did not discharge from the undersurface after being sprinkled with water.

We measured surface layer temperatures to estimate evaporation efficiency and latent heat flux, using the method described above; thermocouple sensors (HOBO U12, produced by Onset Computer Corporation) were used for these experiments. The gravimetries used were precision-balanced (PB-S, produced by METTLER TOLEDO). We measured global solar radiation, air temperature, and humidity through the procedures outlined above, at 1-minute intervals. These

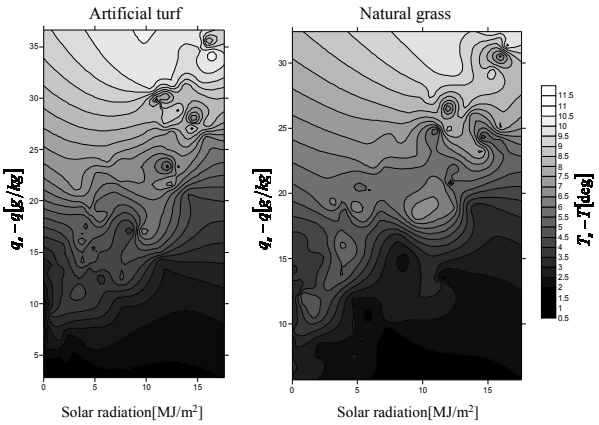

Fig. 7. Relationships of solar radiation, vapor pressure deficit, and differences between surface temperature and air temperature for the artificial turf and natural grass.

experiments were carried out two times each for both artificial and natural grass. Experiments on natural grass used natural grass B, which was cut into 5 cm square samples, the same size as artificial turf samples.

3.5.2 Evaporation from artificial turf and natural grass with soil

Usually, artificial turf fields are installed on top of an impermeable material such as asphalt. However, our proposed artificial turf system field was installed on top of improved soil. Therefore, we compared evaporation from artificial turf to evapotranspiration from natural grass including soil.

Our experimental models (20 x 20 cm) were filled with improved soil, and then surface compaction was allowed, as in a real field. Two types of improved soil were used: Type A (density of 2.849 g/m^3) and Type B (2.886 g/m^3). Densities differed because surface compaction was carried out by hand. In the Type C model, only the surface of river sand was compacted for comparison. These three experimental models were sprinkled with water until they were wet, and then evaporation and evapotranspiration were estimated daily after exposure to the outside air.

In the first condition, experimental models had no artificial turf or natural grass, to estimate the evaporation from improved and non-improved soil; soil evaporation was observed from February–July 2008. Second, evaporation from artificial turf on top of improved soil (Type A) and evapotranspiration from natural grass on top of non-improved soil (Type C) were observed from July–August 2008.

4 RESULTS

4.1 Coefficient of thermal conductivity

Fig. 3 compares measurement results of thermal conductivity by artificial turf, natural grass, and the results of previous research. Artificial turf had less thermal conductivity than natural grass as well as asphalt and concrete, commonly used urban land surfaces. This finding indicates that it is difficult for artificial turf to transfer radiant heat into the ground.

Natural grass probably has greater thermal conductivity than artificial turf because it is never in an absolutely dry condition, and thus it always contains more moisture than artificial turf.

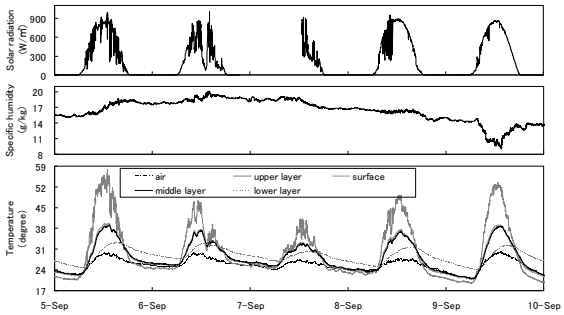

Fig. 8. Time series of solar radiation, specific humidity, and temperature for each layer of the artificial turf, and air temperature from September 4–11, 2008.

Moreover, natural grass layers contain sand and soil, which have higher thermal conductivity than Ecofill. The thermal conductivities of artificial turf and Fine Tuned were similar to those of polyethylene resin and rubber.

4.2 Heat capacity

Fig. 4 shows the time series for the heat capacity of the artificial turf and natural grass from February 29–November 14, 2008. Heat capacity of the artificial turf varied widely from 0.22–12.6 $\times 10^6$ J/m^{3}K, with an average of 2.4 $\times 10^6$ J/m^{3}K. Heat capacity of natural grass was 3.2–4.1 $\times 10^6$ J/m^{3}K, greater than that of the artificial turf. Mean testing revealed no significance. The temperature of artificial turf could be easily altered, and therefore its surface layer temperature was more variable than that of natural grass. This result supports the findings for surface layer temperature discussed above.

The factors affecting the variability of heat capacity of the artificial turf include the moisture content of turf and conditions of air temperature, humidity, wind speed, and cloud amount. Heat capacity of natural grass varied because the natural grass died.

4.3 Albedo

Fig. 5 compares albedo measurements between the artificial turf and the results of previous research. The albedo of an object is the extent to which it diffusely reflects light from the sun. The albedo of the artificial turf was one-quarter that of natural grass. A small albedo indicates a large quantity of input heat. The albedo of artificial turf was smaller than that of asphalt and concrete in urban areas.

4.4 Surface temperature

Fig. 6 shows the time series for solar radiation, specific humidity, and surface temperature of the artificial turf and natural grass, and air temperature from July 14–19, 2008. The surface layer temperature of the artificial turf was about 1°C higher than that of natural grass during daytime. However, during nighttime, the surface layer temperature of the artificial turf was about 2°C lower than that of natural grass.

Fig. 7 shows the relationships among solar radiation, vapor pressure deficit, and differences between surface temperature and air temperature for the artificial turf and natural grass. Blue indicates small differences between surface temperature and air temperature, and red indicates

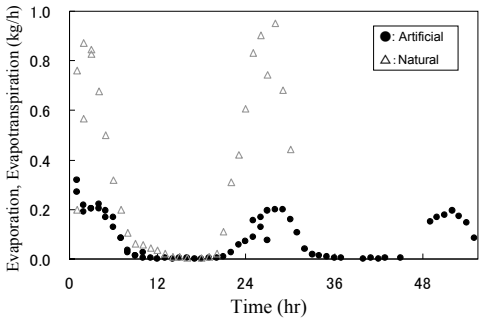

Fig. 9. Time series of evaporation from the artificial turf and evapotranspiration from natural grass.

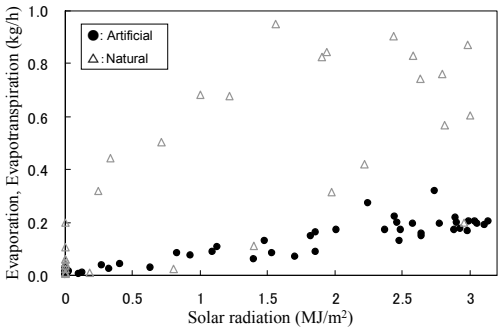

Fig. 10. Relationship between solar radiation and evaporation from the artificial turf, and evapotranspiration from natural grass.

large differences. Data were collected from July 14–19, 2008, and the figure was drawn using the spline interpolation algorithm. The relationships among solar radiation, vapor pressure deficit, and differences between surface temperature and air temperature for the artificial turf and natural grass exhibited a similar global tendency. However, distances between constant-temperature lines were narrow in the figure for artificial turf, indicating that the change in vapor pressure deficit and differences between surface temperature and air temperature were influenced a great deal by solar radiation above the artificial turf.

Fig. 8 shows the time series for solar radiation, specific humidity, and temperature in each layer of the artificial turf and air temperature from September 4–11, 2008. In this study, surface temperature was the temperature at a depth of about 2 cm from the artificial turf surface in the Ecofill layer. The middle layer was between the artificial turf and Fine Tuned, and the lower layer was between Fine Tuned and the improved soil (see Fig. 1).

The temperatures of the artificial turf showed similar behavior qualitatively. However, maximum temperatures of artificial turf had a time lag, and the daily temperature range of the lower layer tended to be smaller than others. This was likely due to the small transfer of radiant heat into the lower layer because of low thermal conductivity. The temperature of the surface and surface layer of the artificial turf were much higher than air temperature during daytime; however, temperatures of all layers were lower than air temperature during nighttime.

4.5 Evaporation

4.5.1 Evaporation from artificial turf and natural grass

Fig. 9 shows the time series for evaporation from the artificial turf and evapotranspiration from natural grass. Maximum evaporation of natural grass was more than four times that of artificial turf. In summary, artificial turf had small levels of evaporation but continued to evaporate longer than natural grass: over a 24-hour period, the accumulated evaporation from artificial turf was about 1.5 mm, and evapotranspiration from natural grass was about 5 mm.

Fig. 10 shows the relationship between solar radiation and evaporation from the artificial turf and evapotranspiration from natural grass. Evaporation from artificial turf increased *pro rata* by solar radiation. However, evapotranspiration from natural grass did not depend on solar radiation. One factor related to this phenomenon was transpiration: the transpiration rate changed by not only climate and/or weather condition, but also by growing condition and moisture content. We

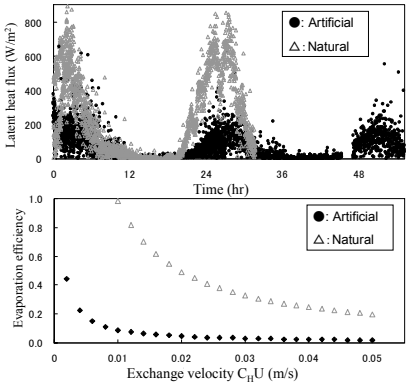

Fig. 11. Latent heat flux and evaporation efficiency of the artificial turf and natural grass.

observed variable growing conditions of natural grass during the experiment; because of this variability, evapotranspiration from natural grass had no relationship to solar radiation.

Fig. 11 shows latent heat flux and evaporation efficiency of the artificial turf and natural grass. Latent heat flux and evaporation efficiency were estimated using the bulk formula. During daytime, latent heat flux of the artificial turf was one-quarter that of natural grass. Therefore, artificial turf had less evaporation compared to natural grass.

4.5.2 Evaporation from artificial turf and natural grass with soil

Fig. 12 shows the time series for rainfall, solar radiation, and evaporation by each experimental model from February 16–March 13, 2008. Evaporation from improved soil and non-improved soil exhibited similar behavior, and evaporation rates from improved soil were almost identical to those from non-improved soil. Immediately after beginning the experiment, evaporation was large regardless of solar radiation. Evaporation was particularly large the day after a rainfall, when moisture content was high and the surface layer held a lot of water.

Fig. 13 shows time series for rainfall, solar radiation, and evaporation or evapotranspiration for each experimental model from July 16–28, 2008. Evaporation from Type A samples covered with artificial turf was one-quarter the evaporation from Type B and Type C samples covered with natural grass. The small evaporation from Type A is attributable to the buffer material, which protected against solar radiation entering the soil and evaporation from the soil, and ensured water retention. Evaporation and evapotranspiration from each model were at the same level 12 days later, although some rainfall fell into models.

5 Summary

We investigated the thermal environmental properties of artificial turf by estimating and comparing the hydrological parameters of artificial turf and natural grass. The surface temperature of the artificial turf was about 2°C lower than that of natural grass during nighttime. Evaporation and albedo of the artificial turf were about one-quarter those of natural grass. Heat capacity and thermal conductivity of the artificial turf were also smaller than those of natural turf. This artificial turf system can be used as an effective countermeasure against hot, humid nights. The artificial turf system has a mitigating effect on radiant heat.

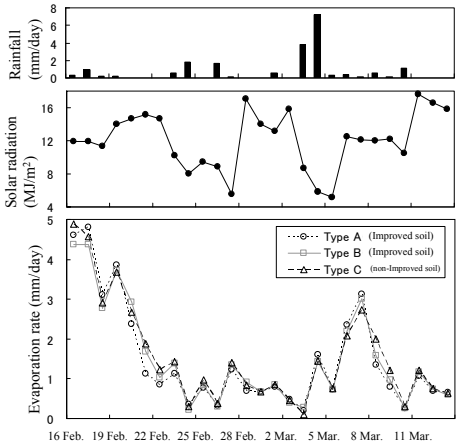

Fig. 12. Time series of rainfall, solar radiation, and evaporation for each experiment model from February 16–March 13, 2008.

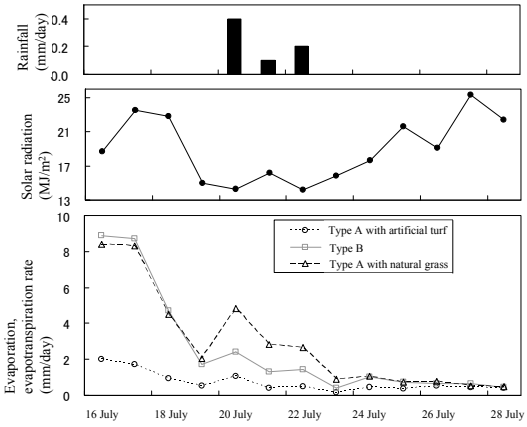

Fig. 13. Time series of rainfall, solar radiation, and evaporation or evapotranspiration from each experiment model from July 16–28, 2008.

6 REFERENCES

Dixon, P.G., Mote, T.L. (2003). "Patterns and Causes of Atlanta's Urban Heat Island–Initiated Precipitation." *Journal of Applied Meteorology*, 42 (9): pp. 1273-1284.

Hirano, Y., Niitsu, K., Ohashi, Y., Ichinose, T. (2004). "Change of surface temperature and heat budget of concrete by the high-albedo paints coating." *Pcoceedings of Annual Conference on Environmental Systems*, JSCE, 32, pp. 183-188.

Ichinose, M., Ishino, H., Hohri, K., and Nagata, A. (2006). "Evaluation of rooftop greening as a method of heat-island reduction based on actual measurement", *J. Environ. Eng. AIJ*, No. 605, pp. 47-54.

Japan Meteorological Agency (2005). "Abnormal climate report 2005." pp.312-323.

Kano, M., Tebakari, T., Kinouchi, T., Sakaki, S., and Yamada, T. (2004). "Social experiment of watering and numerical verification." *Annual Journal of Hydraulic Engineering*, Vol. 48, pp. 193-198.

Kato, T., Tsuchiya, S., Watanabe, A., Ebihara, M., Maemura, Y., Morihisa, S., and Yamada, T. (2007). "Mitigation effect of river cooling action on urban thermal environment." *Proceedings of 2007 Annual Conference,* JSHWR, Vol. 51, pp. 38-39.

Kinouchi, T., and Kobayashi, H. (1999). "Measures for lowering surface temperature of pavementsfor comfortable thermal environment." *Journal of the Japan Society of Civil Engineers*, No. 622, pp. 23-33.

Kondo, J. (1994). *Meteorology of water environment*. Ssakura shoten.

Mikami, T. (2005). "Heat island phenomenon and urban heavy rainfall." *Journal of JAPAN SEWAGE WORKS ASSOCIATION,* Vol. 42, No. 512, pp. 4-6.

Ministry of Environment. (2005). "Reserch on effect of haet island phenomenon on environment 2004"

Murakami, D., and Shimomura, T. (2007). "Examination of comfort by the thermal environment measurementand the subjective experiment on 3 different parts of a green roof." *J. Jpn. Reveget. Tech.*, 33(1), pp. 152-157.

Sugawara, H. (2001). "Heat exchange between urban structures and the atmospheric boundary layer." *Ph.D. Thesis of Tohoku University*.

Tebaakri, T., Watanabe, R., Yamazaki, K., and Inui, M. (2008). "Fundamental study on hydro-meteorological environment over a new-type artificial turf field." *Annual Journal of Hydraulic Engineering*, Vol. 52, pp. 265-270.